

Pulse shape analysis of CUORE-0 bolometers

Daria Santone

*Dipartimento di Scienze Fisiche e Chimiche, Università dell'Aquila, L'Aquila I-67100 - Italy,
INFN - Laboratori Nazionali del Gran Sasso, Assergi (L'Aquila) I-67010 - Italy*

Abstract

The CUORE experiment search the $0\nu\beta\beta$ of ^{130}Te using the bolometric technique. CUORE-0, a CUORE prototype, has been operating in two last years to test the detector performances. The data collected by CUORE-0 makes it ideal to study the bolometer performances for a future improvement of $0\nu\beta\beta$ sensitivity.

1 Introduction

Neutrinoless double beta decay $0\nu\beta\beta$ is a extremely rare process in which a nucleus undergoes two simultaneous beta decays without neutrino emission. Its evidence is a peak in the sum of energy spectrum of two emitted electrons ¹⁾. This process has never been observed but its discovery would demonstrate the lepton number violation and the Majorana nature of neutrino(ν and $\bar{\nu}$ are the

same particle), it also would constrain the neutrino mass absolute scale ²⁾. The Cryogenic Underground Observatory for Rare Events (CUORE) ³⁾, which is in the final stage of construction at LNGS, search the $0\nu\beta\beta$ of ^{130}Te . It is an array of 988 TeO_2 crystals arranged in 19 towers for total mass about 750 kg. One CUORE tower consists in 52 crystals disposed in 13 floors, on each floor there are four TeO_2 crystals, each with a mass of 750 g. CUORE-0, the first CUORE-like tower, has been operating from 2013 to 2015, like CUORE prototype. It demonstrated the efficiency of CUORE assembly line to reduce the α background and that the CUORE crystal energy resolution of 5 keV has been reached ⁴⁾.

The large amount of data collected by CUORE-0 makes it ideal to study in detail the performance of detector response. The aim of my analysis is the characterization of CUORE-0 bolometer response and behavior for a future improvement of $0\nu\beta\beta$ sensitivity.

2 Bolometric technique and TeO_2 bolometer performance

A bolometer is a low temperature calorimeter in which the energy released into the crystal is converted in a thermal signal. It consists in a dielectric crystal, the absorber, and a thermal sensor, that converts the thermal signal in electrical signal ⁵⁾.

A CUORE bolometer ⁶⁾ is a 5x5x5 cm³ TeO_2 crystal equipped with NTD-Ge (Neutron-Transmutation-Doped germanium) thermal sensor, a germanium crystal doped by thermal neutrons. The CUORE bolometer will operate at 10 mK. At this temperature the thermal capacity of TeO_2 is 2.3×10^{-9} J/K. The NTD sensor operates in the Variable Range Hopping regime(VRH): the phonons are responsible of conduction regime and the charge migrate among far impurity sites at Fermi energy. The resistivity is correlated to temperature by the followed relationship:

$$R(T) = R_0 \exp \left[\frac{T_0}{T} \right]^{\frac{1}{2}} \quad (1)$$

where R_0 and T_0 depend on the doping concentration, the value for CUORE-NTD are $R_0 \sim 1\Omega$ and $T_0 \sim 4$ K.

The most important parameter is the detector energy resolution because it determinate the power to discriminate the $0\nu\beta\beta$ peak. CUORE-0 estimated the energy resolution exposing each bolometer to a thoriated tungsten source.

The energy resolution has been evaluated on ^{208}Tl photo-peak (2615 keV) because it is the closest high-statistic signal to the ROI (2527.5 keV). The effective mean FWHM value in CUORE-0 is 4.8 keV (Fig.1).

The energy resolution value is not dominated by electronic noise, so the goal

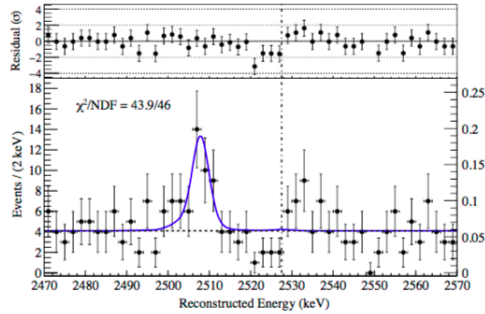


Figure 1: CUORE-0 crystal energy resolution estimated by ^{208}Tl photo-peak

of my analysis is a possible future improvement of energy resolution by a better understanding of bolometer response.

The ideal bolometer response is given by a pulse: the amplitude is proportional to the energy released into the crystal and the decay time is inversely proportional to thermal conductance G . The signal is very slow, so it can be used to search rare events.

Despite this simple model, the actual response is much complex because there are different contribution to the thermal coupling (Fig.2a) ⁷.

The CUORE crystals are housed in a copper structure by PTFE holders, that also are responsible of the thermal coupling between the absorber and heat bath. The NTD is glued to the crystal by a Araldit rapid epoxy and is connected to the electronic by gold wires, responsible of thermal coupling between sensor and heat bath. The electron/phonon decoupling was also observed in the sensor. The electrons and the phonons are at two different temperatures, so there is a thermal conductance between them. Given this different thermal coupling, the thermal model for a CUORE crystal is described in the figure 2b.

Nevertheless, there is not a full thermal model to describe the bolometer response. Finding the different component of CUORE-0 pulses and correlating them to physics parameters will help in developing a better bolometer thermal

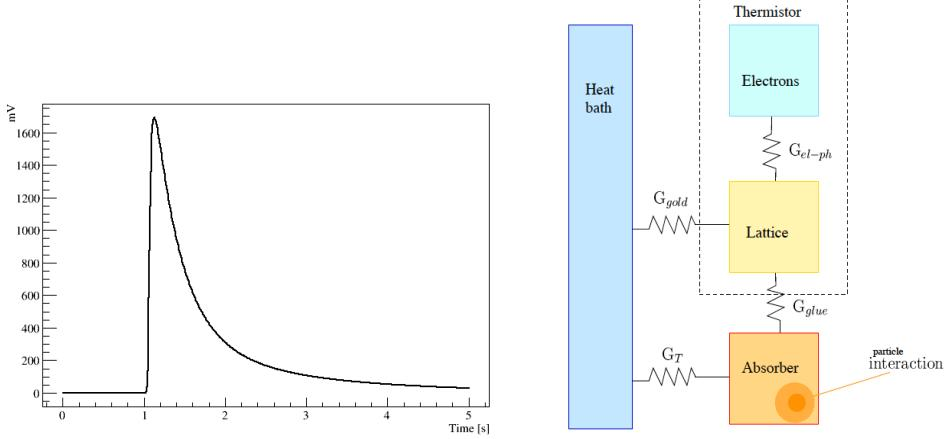


Figure 2: a) An example of CUORE-0 pulse response; b) Thermal model for CUORE-0 bolometers.

model and possible improvement of detector response.

3 Pulse shape analysis

The pulse shape is described by sum of n exponentials and the fit function is given by following form:

$$A_1 \exp \left[\frac{(t_0 - t)}{t_1} \right] + A_2 \exp \left[\frac{(t_0 - t)}{t_2} \right] + \dots - (A_1 + A_2 + \dots + A_n) \exp \left[\frac{(t_0 - t)}{t_r} \right] \quad (2)$$

where t_0 is the trigger time.

The detector response is also influenced by electronic chain effects. They come from the RC filter and 6-poles Bessel filter with a cutoff frequency $\nu_t = 12$ Hz. The RC filter is given by the parasitic capacity c_p of the wiring between the NTD sensor and the electronics. The value of c_p depends on the length of the wires that carry the signal out of cryostat, that is of order of 400 pF. The value of R is the NTD resistance, that is of order 100 M Ω . The 6-poles Bessel filter is used to reduce the aliasing noise in the out-of-band frequency. This filter causes a curvature on the rise of the pulse and a delay of the signal. This effects are simulated by the sigmoid function to simplify the fit computing program.

The fit function is given by:

$$\frac{1}{1 + \exp[-\text{sigma}(t - s_0)]} \times \text{CONV} \left[\left(\frac{1}{RC} \exp \left[-\frac{t}{RC} \right] \right), \text{pulseshape}(A_i, t_r, t_{d_i}) \right] \quad (3)$$

where the sigmoid parameters are the curvature on the rise (*sigma*) and the delay of the pulse (*s*₀).

The first step is to define how many time constants describe the pulse shape. The figure 3 shows two examples fit of 2615 keV γ -ray pulse. The one on the left is a sum of four exponentials (one rise plus three decays) and the one on the right is a sum of five exponentials (one rise plus four decays).

The fit residuals show that the five exponentials fit describe much better the pulse shape, especially in the first part of the pulse (fig.4).

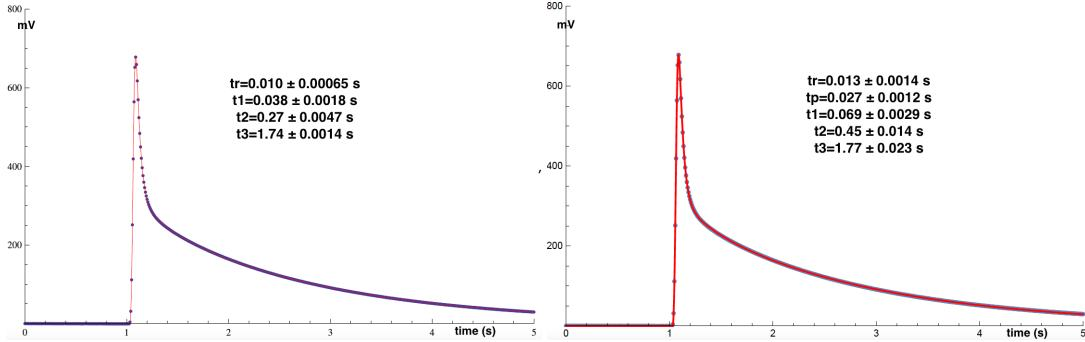


Figure 3: a) Four exponentials fit b) Five exponentials fit

It also observed that the first time decay *t*_p is correlated to a platinum contamination present in the TeO₂ crystals. This contamination originates during TeO₂ crystals growth, because the crucibles are made of platinum foil. The platinum contamination is estimated looking at the ¹⁹⁰Pt peak counting rate in the energy range 3200 - 3400 keV for each crystal ⁸⁾. The time constant *t*_p shows up only for ¹⁹⁰Pt rate upper than 150 count/kg/years. At lower rate *t*_p is not necessary to describe the pulse shape, although the response is influenced by platinum heat capacity. In fact the estimation of *t*_r, *t*₁ and *t*₂ is correlated to platinum rate (Fig.5).

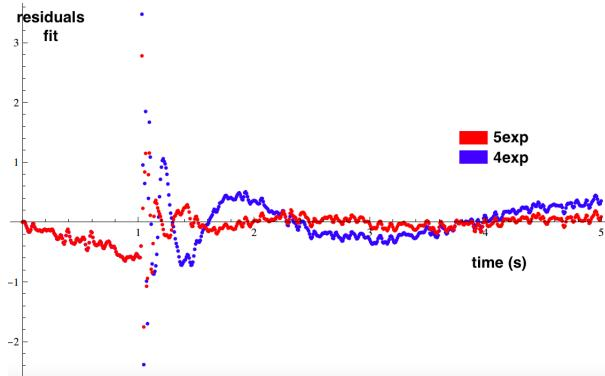


Figure 4: Comparison between four and five exponential fit residuals

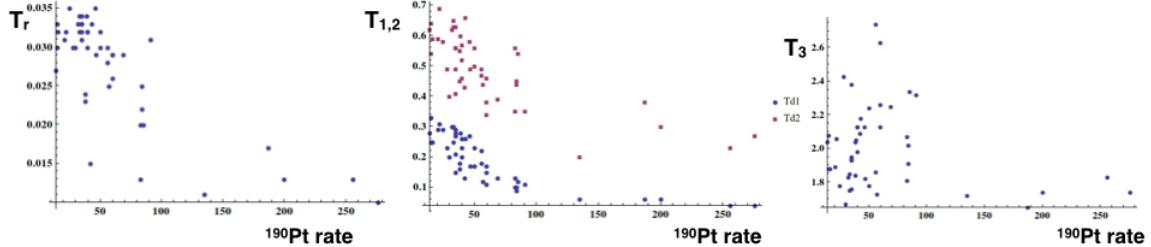


Figure 5: Time constant estimation vs Platinum rate.

References

1. J. D Vergados, H. Ejiri, F. Simkovic, Rep. Prog. Phys. 75 (2012).
2. A. Strumia, F. Vissani, arXiv.org/abs/hep-ph/0606054 (2010)
3. C. Arnaldoldi *et al.*, Nucl.Instr.Meth. (2004)
4. CUORE Collaboration, Phys.Rev.Lett.115 no.10, 102502 (2015)
5. K. Petzl, Nuclear Instruments and Methods in Physics Research (2000)
6. CUORE Collaboration, arXiv:1604.05465 (2016)
7. M. Carattoni, M. Vignati, Journal of Instrumentation, Vol.6 (2011)
8. F. Alessandria *et.al.*, Astropart.Phys.35, 893-849 (2012)